15TH IEA HEAT PUMP CONFERENCE
MAY 26–29, 2026 | HOFBURG
VIENNA 2026
DECARBONISATION THROUGH INNOVATION

Considering groundwater flow in BHEs design through an evolution of the ASHRAE sizing method

Carlo Leali[a], Adriana Angelotti[b*]

[a]School of Industrial Engineering, Politecnico di Milano, v. La Masa 32, 20156, Milano, Italy
[b]Energy Department, Politecnico di Milano, v. Lambruschini 4A, 20156, Milano, Italy

Abstract

According to literature, the presence of groundwater flow enhances Borehole Heat Exchangers operation, since an advection mechanism is added to conduction. Therefore, if the effect of groundwater flow was included in the design phase, it is expected that it would result in smaller borefields and lower excavation costs. However, simple BHE sizing methods accounting for groundwater flow are presently lacking.
In this paper we propose to modify the well-known sizing method from the ASHRAE standard to improve accuracy and include the medium and long-term groundwater impact. The procedure exploits the reformulation of the ASHRAE sizing equation and of the so-called Temperature Penalty in terms of g-functions. To identify the most suitable analytical solutions to calculate the medium and the long-term ground thermal response, depending on the relevant distances and heat transfer mechanism, the behavior of the main analytical solutions for heat sources is first discussed. Then the Finite Line Source and the Moving Finite Line Source g-functions are implemented in the sizing equation for the case without and with groundwater flow, respectively.
To illustrate the new methodology, a series of case studies is generated by varying the ground loads, the Darcy flow velocity and direction, as well as the borefield characteristics. The borefield sizings resulting from the new method are then compared with those obtained by applying the original ASHRAE method. The comparison showed that Darcy velocity equal to 10^{-7} m/s can be considered the minimum threshold above which advection effect cannot be neglected. The beneficial influence of the groundwater flow on the BHEs sizing is more pronounced for small borehole spacing and unbalanced heating and cooling loads in the ground.

Keywords: BHE; ASHRAE sizing method; groundwater flow;Finite Line Source; Moving Finite Line Source.

1. Introduction

The design of Borehole Heat Exchangers (BHE) can nowadays be performed through different tools, ranging from simplified spreadsheet methods to more accurate dynamic simulation tools [1]. The sizing equation proposed by Kavanaugh and Rafferty [2] and adopted by ASHRAE standard is one the most widespread simplified methods. It is based on the representation of the ground load profile as the superposition of three primary pulses (hourly, monthly and yearly) and on the use of the Infinite Cylindrical Source (ICS) solution to calculate the ground thermal response at the three key time scales. Long-term interactions among boreholes as well as deviations from the ICS solution are taken into account through the so-called Temperature Penalty correction. Since its original proposal, several improvements to the ASHRAE method have been suggested, either focusing on a more accurate evaluation of the Temperature Penalty [3-6] or aiming to a more precise evaluation of short-term thermal response and long-term interactions among boreholes [7]. To the best of the Authors' knowledge, apart from a recent update of the GHE Analysis tool, no attempt was made to date to include groundwater flow effect in simplified sizing methods and in particular in the ASHRAE sizing equation. Yet the impact of advection in BHE performance has been proved by many studies, among which [8,9]. In this study, by exploiting the reformulation of the ASHRAE sizing equation in terms of g-functions as

* Corresponding author. *E-mail address:* adriana.angelotti@polimi.it

in [7, 10] and the Moving Finite Line Source (MFLS) analytical model [11], a methodology is proposed to consider the influence of the groundwater flow in the BHE design.

2. Methodology

2.1. Reformulation of the ASHRAE sizing equation in terms of G-functions

In the ASHRAE standard sizing method [2] the total required length of the borefield is found through the following equation:

$$L_{H/C} = \frac{R_y \cdot Q_{gy} + R_m \cdot Q_{gmH/C} + (R_h + R_b) \cdot Q_{ghH/C}}{T_\infty - T_{mfH/C} - T_p} \tag{1}$$

where:

- Q_{gy}, Q_{gm}, Q_{gh} are the yearly, monthly and hourly ground loads, the latter two being different for heating (H) or cooling (C) operation,
- R_y, R_m, R_h are the ground thermal resistances related to the yearly, monthly and hourly heat loads,
- R_b is the BHE thermal resistance,
- T_∞ is the ground undisturbed temperature,
- T_{mf} is the mean fluid temperature in the BHE,
- T_p is the temperature penalty.

Eq. (1) is applied both for heating and cooling, resulting in total lengths L_H and L_C, and the final size is chosen as the maximum between them:

$$L = max\{L_H, L_C\} \tag{2}$$

The temperature penalty is found by estimating through the Infinite Line Source (ILS) solution Q_{stored}, namely the energy stored during 10 years in a hollow cylindrical volume of ground around a borehole. The inner radius is half the distance B between two boreholes, and the maximum radius is conventionally 10 m. By assigning Q_{stored} to a ground parallelepiped with base BxB and height L a "base" temperature alteration T_{p4} in the ground is found through Eq. (3):

$$T_{p4} = \frac{Q_{stored}}{C_g B^2 L} \tag{3}$$

where C_g is the ground volumetric capacity. T_{p4} is subsequently corrected through the *TPF* factor that takes into account the number of boreholes with 1, 2, 3 and 4 neighbors, as in the following equation:

$$T_p = T_{p4} \cdot TPF \tag{4}$$

The physical meaning of the sizing equation (1) can be understood by following the approach in [10]. By exploiting time superposition, the average borehole wall temperature T_b at time t_n can be expressed as:

$$T_b(t_n) = T_\infty - \frac{1}{\lambda_g} \sum_{i=1}^{N} (q_i - q_{i-1}) \cdot G(t_n - t_{i-1}) \tag{5}$$

where:

- λ_g is the ground thermal conductivity,
- q_i is the step heat pulse starting at time t_i,
- G is the non-dimensional ground response at the borehole wall or g-function.

By introducing the time variable τ_i representing the time passed since the last load step:

$$\tau_i = t_n - t_{i-1} \tag{6}$$

Eq. (5) can be reformulated as:

$$T_b(t_n) = T_\infty - \frac{q_n}{\lambda_g} G(\tau_N) - \sum_{i=1}^{N-1} \frac{q_i}{\lambda_g} \cdot [G(\tau_i) - G(\tau_{i+1})] \tag{7}$$

The mean fluid temperature T_{mf} can be related to the average borehole wall temperature through the formula:

$$T_{mf} = T_b - R_b \cdot q_n \tag{8}$$

And by inserting Eq. (7) into Eq. (8) we obtain:

$$T_{mf}(t_n) = T_\infty - q_N \left[R_b + \frac{G(\tau_N)}{\lambda_g}\right] - \sum_{i=1}^{N-1} \frac{q_i}{\lambda_g} \cdot [G(\tau_i) - G(\tau_{i+1})] \tag{9}$$

The $N = 3$ main load steps considered in Eq. (1) are the hourly, monthly and yearly ones:

$$q_{gh} = \frac{Q_{gh}}{L} \quad q_{gm} = \frac{Q_{gm}}{L} \quad q_{gy} = \frac{Q_{gy}}{L} \tag{10}$$

corresponding to $\tau_3 = 6$ h, $\tau_2 = (6$ h + 1 m) and $\tau_1 = (6$ h + 1 m + 10 y). By inserting the ground loads in Eq. (10) into Eq. (9) the following equation is found:

$$T_{mf} = T_\infty - \frac{Q_{gh}}{L}\left[R_b + \frac{G(\tau_3)}{\lambda_g}\right] - \frac{Q_{gm}}{L}\frac{[G(\tau_2)-G(\tau_3)]}{\lambda_g} - \frac{Q_{gy}}{L}\frac{[G(\tau_1)-G(\tau_2)]}{\lambda_g} \tag{11}$$

Now the choice at the basis of the original ASHRAE sizing equation (Eq. 1) is to use the g-function for a single ICS (namely $G_{ICS,s}$) at the three times, and to include all the deviations in the ground response to the long-term pulse related to the simplified representation of the BHE as an ICS (such as axial effect due to the finite depth of the BHEs), and to the interference among neighboring boreholes, in a temperature correction T_p. The yearly, monthly and hourly thermal resistances in Eq. (1) are thus defined as:

$$R_y = \frac{G_{ICS,s}(\tau_1)-G_{ICS,s}(\tau_2)}{\lambda_g} \qquad R_m = \frac{G_{ICS,s}(\tau_2)-G_{ICS,s}(\tau_3)}{\lambda_g} \qquad R_h = \frac{G_{ICS,s}(\tau_3)}{\lambda_g} \tag{12}$$

while the temperature penalty can be expressed as:

$$T_p = \frac{Q_{gy}}{L}\frac{[G_{true}(\tau_1)-G_{ICS,s}(\tau_1)]}{\lambda_g} \tag{13}$$

where $G_{true}(\tau_1)$ represents the "true" non-dimensional average thermal response of the ground at the borehole wall in a given borefield. Inserting Eqs. (12) and (13) into Eq. (11) gives the following equation:

$$T_{mf} - T_\infty - T_p = -\frac{1}{L}\left[\, Q_{gh}(R_b + R_h) + Q_{gm}R_m + Q_{gy}R_y\right] \tag{14}$$

that, solved for L, returns the classical form of the sizing equation Eq. (1). However, this formalism points out the possibility to define the three ground thermal resistances in a more general way in terms of generic g-functions:

$$R_y = \frac{G(\tau_1)-G(\tau_2)}{\lambda_g} \qquad R_m = \frac{G(\tau_2)-G(\tau_3)}{\lambda_g} \qquad R_h = \frac{G(\tau_3)}{\lambda_g} \tag{15}$$

Provided that relevant long-term effects are accounted for by a proper choice of $G(\tau_1)$, the temperature penalty correction can be avoided, and the sizing equation becomes:

$$L = \frac{R_y \cdot Q_{gy} + R_m \cdot Q_{gm} + (R_b + R_h) \cdot Q_{gh}}{T_\infty - T_{mf}} \tag{16}$$

Eq. (16) is the sizing equation adopted in this study as it opens the door to the possibility to include groundwater flow effect through a suitable choice of thermal resistances.

2.2. Choosing the best g-functions for each time scale, distance and heat transfer mechanism

The implementation of Eq. (16) was preceded by an analysis of the behavior of the available analytical solutions for simulating heat sources in the ground. The ranges of the relevant ground properties, the geometric parameters of the BHE and the radial distance considered in this analysis are reported in Table 1.

Table 1. Range of variations of ground and geometric parameters adopted for the comparison among analytical solutions

Parameter	Unit	Min value	Max value
Ground volumetric capacity C_g	MJ/(m^3.K)	2	3
Ground thermal conductivity λ_g	W/(m·K)	1.5	3.5
Ground thermal diffusivity α_g	m^2/s	$5.0 \cdot 10^{-7}$	$1.75 \cdot 10^{-6}$
Borehole radius r_b	m	0.05	0.1
Borehole depth H	m	50	150
Radial distance from the source r	m	0.05	10

In the preliminary analysis the ICS solution at the time scales and distances that are relevant for the sizing method is compared with the ILS, the Finite Line Source (FLS) [12] and the Moving Finite Line Source (MFLS) [11]. Both FLS and MLFS are averaged over the source length H and the MFLS is also averaged over the angular coordinate.

The plot of the g-functions of the ILS and ICS models as functions of the Fourier number $Fo_b = \alpha_g t / r_b^2$ and for different dimensionless radial distances r/r_b is presented in Fig.1. By letting ground thermal diffusivity and borehole radius vary in typical ranges (Table 1), Fo_b numbers corresponding to the key time scales τ_1, τ_2 and τ_3 vary accordingly. The Fo_b ranges correspondent to the mentioned time intervals are then also indicated in the top part of Fig.1.

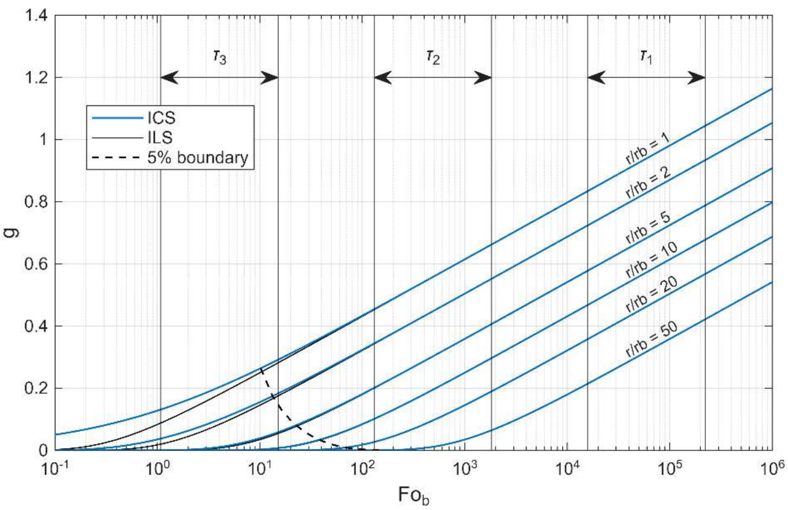

Figure 1. g-function obtained with ICS and ILS versus Fo_b for different ratios r/r_b. The line corresponding to 5% difference between the two as defined in [13] is shown, as well as the range of Fo_b that corresponds to the time scales τ_1, τ_2 and τ_3

In agreement with literature [14], the plot shows that ICS and ILS disagree only at short times and small distances, while there is no difference between them in the medium and long term at any distance. This confirms that replacing the ICS with the ILS at larger times scales would be useless. Moreover, since the g-function corresponding to typical borehole to borehole spacing (e.g. $r/r_b = 50$) is almost null at τ_3, there is actually no need to take into account thermal interactions among boreholes at such time scale.

The FLS g-functions are compared with the ILS ones in Fig. 2. In this case the source depth H is used as the characteristic length in Fourier number i.e. $Fo_H = \alpha_g t / H^2$ and in the non-dimensional radial distance $R = r/H$. The three curves corresponding to the higher R values are obtained for r = 5 m and H = 50 m, r = 5 m and H = 150 m, r = 10 m and H = 150 m. The two curves with lower R are obtained with r = 0.1 m, H = 50 m and r = 0.05 m, H = 150 m. The 5% difference line defined by Conti [13] is also plotted in Fig. 2 to help identifying when and where axial effects caused by the finite length of the source are relevant. They are null at the short time scale (Fo_H corresponding to τ_3), start to be noticeable at borehole spacings and medium time scales (Fo_H corresponding to τ_2), and become important at all distances for large time scales (Fo_H corresponding to τ_1). Fig. 2 suggests that the FLS applied to the borefield should be used to calculate $G(\tau_1)$ and $G(\tau_2)$.

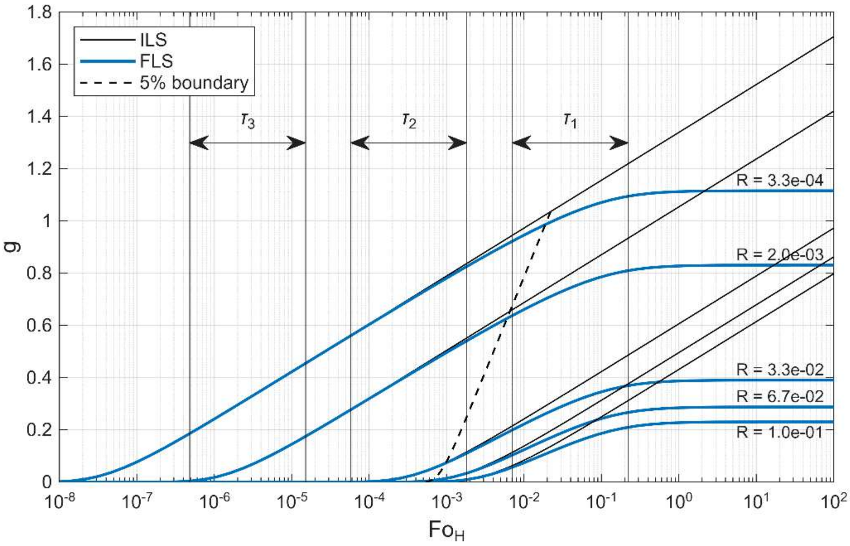

Figure 2. g-function obtained with ILS and the FLS versus Fo_H for different ratios $R = r/H$. The line corresponding to 5% difference between the two as defined in [13] is shown, as well as the range of Fo_H that corresponds to the time scales τ_1, τ_2 and τ_3

In order to discuss the impact of groundwater flow, the g-functions obtained with the MFLS solution are plotted together with the FLS ones in Fig. 3 and 4 as functions of Fo_H. The MFLS curves are generated considering the minimum and maximum Darcy velocities in Table 1 and H = 150 m. Fig. 3 refers to $R = 3.33 \cdot 10^{-4}$ while Fig. 4 to $R = 3.33 \cdot 10^{-2}$ and are thus representative of borehole radius and borehole spacing respectively. The curves are labelled according to the Péclet number $Pé_H = C_w v_D H/\lambda_g$, where C_w is the water volumetric heat capacity and v_d is Darcy velocity. It can be noticed that for small R the MFLS deviates from the FLS at small time scales only at very high Péclet, namely for high Darcy velocity and short BHE. The larger the time, the lower the Darcy velocity leading to remarkable effects, so that not only at τ_3 but also at τ_2 the MFLS would be preferrable. For large R, groundwater effects are important at τ_2 only for the very high flow and short BHE, while they are always important at τ_1. These considerations imply that when groundwater flow is present, MFLS should be used to calculate $G(\tau_2)$ and $G(\tau_1)$, in both cases considering the self and the interaction parts.

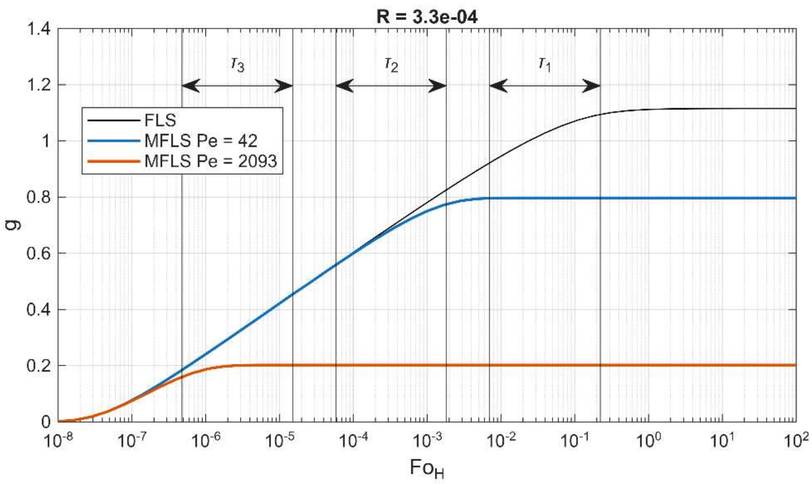

Figure 3. g-functions obtained with FLS and MFLS versus Fo_H for different $Pé_H$, with $R = 3.33 \cdot 10^{-4}$

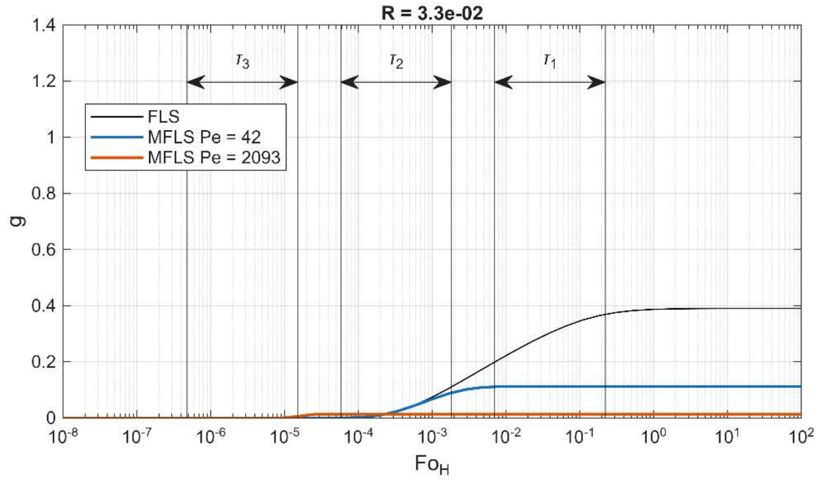

Figure 4. g-functions obtained with FLS and MFLS versus Fo_H for different $Pé_H$, with $R = 3.33 \cdot 10^{-2}$

2.3. Implementing the G-functions-based sizing method

Following the discussion in section 2.2, the sizing equation Eq. (16) is implemented by choosing the following g-functions at the three time scales:

$$G(\tau_3) = G_{ICS,s}(\tau_3) \qquad G(\tau_2) = \begin{cases} G_{FLS,s}(\tau_2) & v_D = 0 \\ G_{MFLS,s}(\tau_2) & v_D > 0 \end{cases} \qquad G(\tau_1) = \begin{cases} G_{FLS,t}(\tau_1) & v_D = 0 \\ G_{MFLS,t}(\tau_1) & v_D > 0 \end{cases} \tag{17}$$

where, for a given model, the total g-function G_t is defined as the sum of the single source g-function G_s, accounting for the effect of the source at its own borehole radius, and the multiple sources g-function G_i, accounting for the average effect of the other BHEs in the field at the borehole radius, as in Eq. (18):

$$G_t = G_s + G_i \tag{18}$$

With reference to the classification of g-functions according to the kind of boundary conditions adopted to generate them [15], we point out that the ones implemented here are generated by assuming a heat rate both uniform along the length and equal for all boreholes (BC type I). In this regard, the G-FLS method presented here is different from [7], where BC type III FLS g-functions are used.

By recalling Eq. (15), it is remarked that the calculation of the hourly thermal resistance R_h is the same in the classical ASHRAE sizing method and in the here proposed G-functions-based sizing method. In turn, the monthly and yearly resistances R_m and R_y are now calculated in a different way: in the purely conductive case they take into account axial effects of the BHE and thermal interactions among boreholes, so that the temperature penalty correction is no longer necessary. In the case of combined conduction and advection they also take into account the effect of groundwater flow through MFLS g-functions.

This approach as well as the classical ASHRAE one were implemented in a Matlab script. The inputs of both methods are the ground loads (Q_{gy}, Q_{gmH}, Q_{gmC} Q_{ghH}, Q_{ghC}), the ground properties ($\lambda_g, \alpha_g, T_\infty$) and eventually the aquifer velocity and direction (v_D, ϕ), the thermal-fluid temperatures (T_{mfH}, T_{mfC}) and the BHE properties (r_b, single/double U pipe configuration, grout conductivity λ_{gr}). It is required to input also the borehole spacing B and the maximum value for the borehole depth H_{max}.

The sizing requires an iterative procedure:

- in the classical approach of Eq. (1) the first calculation is performed neglecting T_p; the resulting total length L_0 defines the necessary number of BHEs with depth close to H_{max}, and a first rectangular layout is created by assuming the distance B; based on this layout, T_p is estimated and a new total length L is derived;
- in the G-functions based approach of Eq. (16) the first calculation is performed neglecting the BHEs interaction contribution, namely adopting $G_{FLS,t}(\tau_1) = G_{FLS,s}(\tau_1)$ or $G_{MFLS,t}(\tau_1) = G_{MFLS,s}(\tau_1)$ in the absence or presence of groundwater flow; the resulting total length L_0 is then used to calculate the necessary number of BHEs with depth close to H_{max}, and a first rectangular layout is created by

assuming the borehole spacing B; based on this layout $G_{FLS,i}(\tau_1)$ or $G_{MFLS,i}(\tau_1)$ are calculated and the total length is updated.

In both cases the total length L_k calculated at step k is compared with the one derived at the previous iteration step L_{k-1} and the process ends when the difference between them is lower than a set tolerance.

2.4. Comparison between the classical ASHRAE method and the G-functions-based method

A series of cases was generated in order to compare the classical ASHRAE method and the improved G-functions-based one. Real sizing problems start from the building heating and cooling demand, that can be summarized by the design heating and cooling loads (Q_H, Q_C) and the Partial Load Factors for the design months (PLF_{mH}, PLF_{mC}) and for the whole year (PLF_{yH}, PLF_{yC}). The ground loads required by the sizing procedure can be obtained from the building parameters and from the heat pump design (COP_d, EER_d) and mean seasonal coefficients (COP_{ms}, EER_{ms}) through the following equations:

$$Q_{ghH} = Q_H \cdot \left(1 - \frac{1}{COP_d}\right) \qquad Q_{ghC} = Q_C \cdot \left(1 + \frac{1}{EER_d}\right) \tag{19}$$

$$Q_{gmH} = Q_H \cdot \left(1 - \frac{1}{COP_d}\right) \cdot PLF_{mH} \qquad Q_{gmC} = Q_C \cdot \left(1 + \frac{1}{EER_d}\right) \cdot PLF_{mC} \tag{20}$$

$$Q_{gy} = Q_H \cdot \left(1 - \frac{1}{COP_{ms}}\right) \cdot PLF_{yH} + Q_C \cdot \left(1 + \frac{1}{EER_{ms}}\right) \cdot PLF_{yC} \tag{21}$$

In order to easily generate different building load profiles, the following two parameters are introduced, namely the maximum absolute building design load Q_d and the load imbalance β:

$$Q_d = max(Q_H, |Q_C|) \qquad \beta = \frac{Q_H + Q_C}{Q_d} \tag{22}$$

It can be noticed that β spans from -1 to 1 and synthetizes the degree of asymmetry between heating and cooling design loads, where negative values correspond to cooling dominated cases since $Q_C < 0$. Q_d and β were thus adopted instead of Q_H and Q_C. In particular, by combining Eq. (21) with Eq. (22), the yearly net ground load Q_{gy} can be rewritten and normalized with respect to Q_d, resulting in Q_{gy}*:

$$Q_{gy}^* = \frac{Q_{gy}}{Q_d} = \begin{cases} (\beta + 1)\left(1 - \frac{1}{COP_{ms}}\right) PLF_{yH} - \left(1 + \frac{1}{EER_{ms}}\right) PLF_{yC} & -1 \le \beta < 0 \\ \left(1 - \frac{1}{COP_{ms}}\right) PLF_{yH} + (\beta - 1)\left(1 + \frac{1}{EER_{ms}}\right) PLF_{yC} & 0 \le \beta \le 1 \end{cases} \tag{23}$$

In order to generate the case studies, an initial distinction was decided between constant inputs (Table 2) and varied ones (Table 3). It can be noticed that the ranges for the ground thermal and hydrogeological properties in Table 3 are the same as in Table 1.

Table 2. Constant input parameters for the case studies

Parameter	Unit	Value
Undisturbed ground temperature T_∞	°C	13
Mean fluid temperature heating/cooling mode T_{mfH}/T_{mfC}	°C	4/30
Design COP_d/EER_d	-	3.8/3.3
Mean seasonal COP_{ms}/EER_{ms}	-	4.7/4.1
Pipe thermal conductivity λ_p	W/(m·K)	0.35
Grout thermal conducitivity λ_{gr}	W/(m·K)	1.7

The range for the maximum building design load Q_d (10 kW −1 MW) covers small and large buildings demands. The Partial Load Factors range was chosen to represent typical scenarios in Northern Italy climate. A preliminary sensitivity analysis performed on the 14 parameters reported in Table 3 allowed to identify the ones that mostly influence the total borehole length L as the ground thermal conductivity, the Darcy velocity, the maximum absolute design load, the load imbalance and the borehole spacing. Following these outcomes, to limit the overall number of cases to be generated, only some of the 14 parameters were actually allowed to vary (bold parameters in Table 3). The values assumed in the case studies are reported in the last column of Table 3, resulting in 261 conduction cases and 783 conduction and advection cases.

Table 3. Ranged input parameters for the case studies

Parameter	Unit	Sensitivity analysis range		Case studies values
		Min value	Max value	
Ground volumetric capacity C_g	MJ/(m^3.K)	2	3	2
Ground thermal conductivity λ_g	W/(m·K)	1.5	3.5	2.4
Darcy velocity v_D	**m/s**	**10^{-7}**	**$5 \cdot 10^{-6}$**	**10^{-7}, $5 \cdot 10^{-7}$, 10^{-6}**
Darcy flow direction ϕ	°	0	90	0
Maximum absolute design load Q_d	**kW**	**10**	**10^3**	**80, 400, 800**
Load imbalance β_l	**-**	**-1**	**1**	**-0.8 - 0.8 step 0.057**
Monthly partial load factor heating PLF_{mH}	-	0.2	0.4	0.25
Monthly partial load factor cooling PLF_{mC}	-	0.2	0.4	0.25
Seasonal partial load factor heating PLF_{yH}	-	0.05	0.15	0.15
Seasonal partial load factor cooling PLF_{yC}	-	0.05	0.15	0.15
Borehole radius r_b	m	0.05	0.1	0.075
Maximum borehole depth H_{max}	m	50	150	100
Borehole spacing B	**m**	**5**	**10**	**5, 7.5, 10**
Layout Aspect Ratio AR	-	1	4	1

3. Results

3.1. Comparison between the classical ASHRAE method and the G-FLS method

As a first step, the original ASHRAE sizing method and the G-functions-based one are compared assuming null groundwater flow, namely in the hypothesis of pure conduction heat transfer in the ground.

The total boreholes length L obtained with the two methods is reported in Fig. 5 as a function of the normalized net annual ground load $Q_{gy}*$ (Eq. (23)) for different values of the maximum design load Q_d (Eq. (22)) and borehole spacing B. First, we observe from Eq. (23) that when building design loads are perfectly balanced ($\beta = 0$) the net annual ground load is not null, rather in this case $Q_{gy}* = -0.07$.

For given Q_d and B the minimum of the required length L as function of $Q_{gy}*$ reflects the switching from $L = L_c$ (decreasing part of the curve, cooling dominated condition) to $L = L_h$ (increasing part of the curve, heating dominated condition) for both sizing methods. Fig. 5 shows that the G-FLS sizing is more sensitive to the net annual ground load with respect to ASHRAE sizing. Such sensitivity is larger for greater maximum design load Q_d and for lower borehole spacing B.

The right part of Fig. 5 reports the relative difference between the two sizing lengths defined as:

$$e_L = \frac{L_{FLS} - L_{ASH}}{L_{ASH}} \tag{24}$$

It can be noticed that the relative difference is small for low $Q_{gy}*$, low Q_d and large B. However, it becomes significant for large, unbalanced ground loads, large building loads and medium to small borehole distances. This behavior reflects the better estimation in the G-functions-based sizing through field FLS solutions of the axial effects and of the interference among boreholes in the long term, although the BC-I type FLS g-functions used here may overestimate thermal interactions effects with respect to BC-II and III type [15]. In general, the G-functions-based method predicts larger borefield sizes compared to ASHRAE original method.

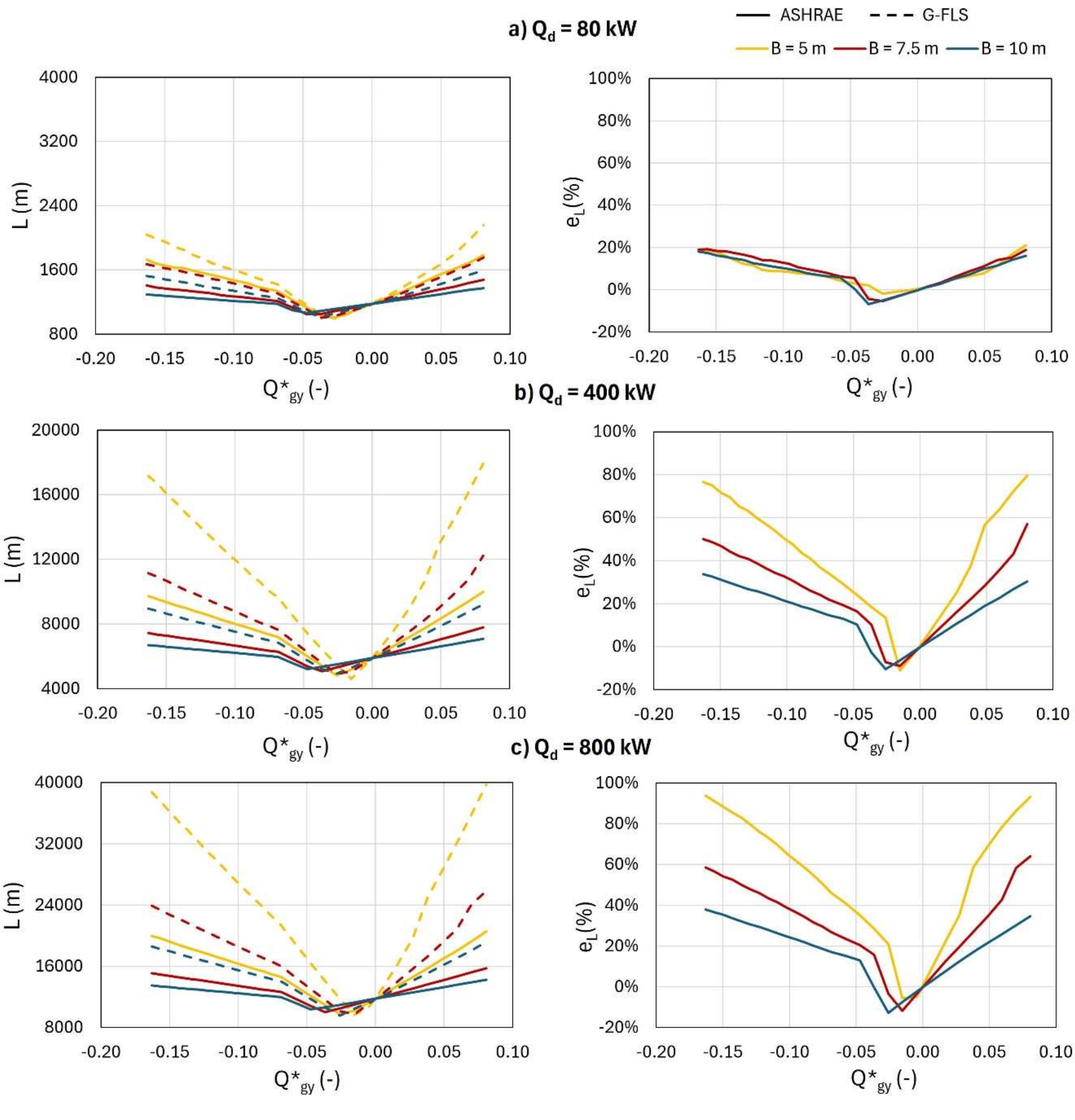

Figure 5. Comparison between the ASHRAE and the FLS-G method sizings: total borehole length L (left) and relative difference in the total length (right) versus normalized ground load Q_{gy}* for maximum design load a) 80 kW, b) 400 kW, c) 800 kW and spacing *B*

3.2. Comparison between the G-FLS and the G-MFLS method

As a second step, the impact of groundwater flow on the design of the borefield is assessed by applying the G-functions-based method with either the FLS or the MFLS field g-functions. The resulting total borefield lengths are compared in Fig. 6, where they are plotted as functions of the normalized net annual ground load Q_{gy}*, for different values of the maximum design load Q_d and borehole spacing *B*. Different curves are plotted for each Darcy velocity reported in Table 3. If groundwater flow is considered, when the Darcy velocity is low (v_d = 10^{-7} m/s), the trend of the total length versus Q_{gy}* is similar to the one obtained assuming no flow. On the contrary, at medium and large Darcy velocity *L* becomes almost constant with Q_{gy}*, although the switching from the cooling dominated to the heating dominated situations is always noticeable. This behavior can be explained in terms of a very small value of the long-term thermal resistance R_y that, according to Eq. (15), is related to the difference between $G(\tau_1)$ and $G(\tau_2)$. For high groundwater velocity the steady state regime is approached both for τ_2 and τ_1. Following, $G(\tau_1) \approx G(\tau_2)$, $R_y \approx 0$ and thus the sizing equation Eq. (16)

becomes poorly sensitive to q_{gy}. At medium and large Darcy velocity the sizing becomes also less sensitive to the borehole spacing, as can be noticed by passing from left to right in Fig. 6.

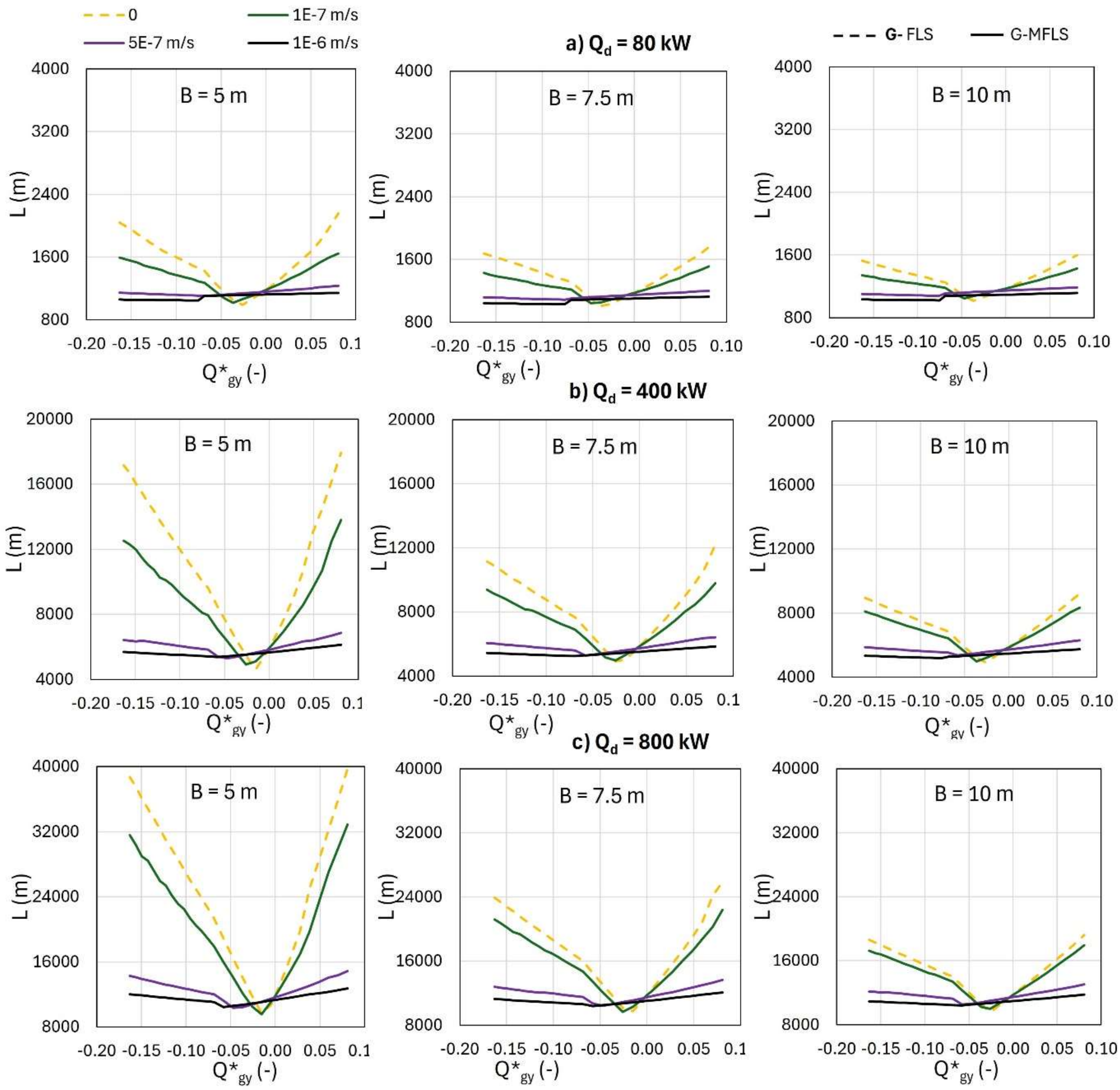

Figure 6. Comparison between the FLS and the MFLS G-functions method sizings: total borehole length L (left) versus normalized ground load Q_{gy}* for different maximum design load a) 80 kW, b) 400 kW and c) 800 kW, borehole spacings *B* and Darcy velocities.

The relative difference e_L between MFLS and FLS sizings is plotted in Fig. 7, where the generally negative values mean that a smaller size of the borefield is obtained when considering groundwater flow. Positive values often found for slightly negative values of Q_{gy}* can be traced back to the different sensitivity of the two methods to this parameter. As already observed in Fig. 6, the G-FLS method exhibits a transition region in which a minimum in *L* is reached. In contrast, at higher values of v_D, the G-MFLS method produces a monotonic curve for *L* over the same interval, with values consistently higher than those of the G-FLS method.

The plots of e_L in Fig. 7 clearly indicate that the difference between the models remains stable and below 20% for the lower bound of v_D. However, as the aquifer velocity increases, the discrepancy becomes more pronounced, highlighting that significant reduction in the borefield size can be achieved for every design load Q_d, and especially for large ground unbalanced load and small borehole spacing.

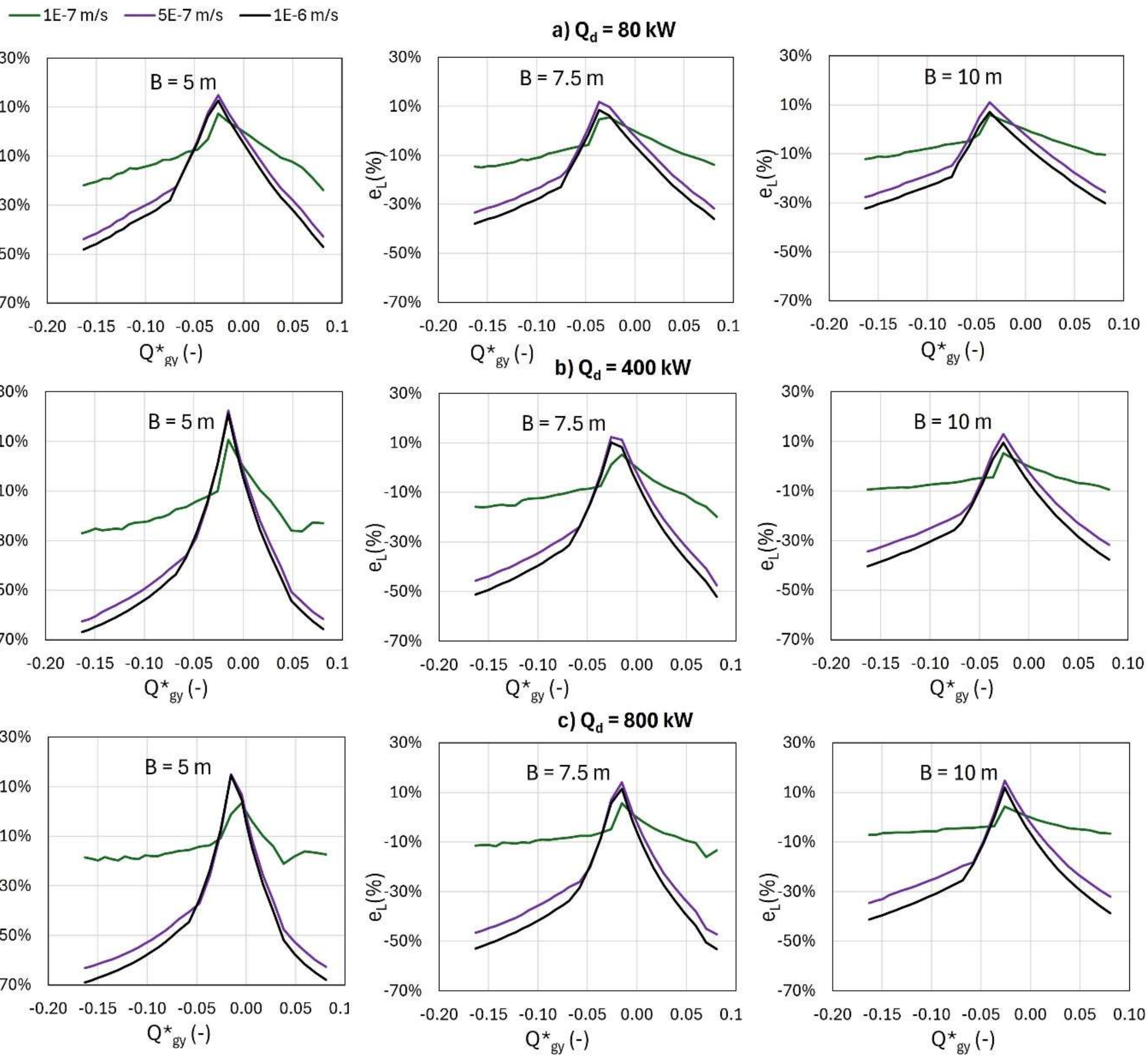

Figure 7. Relative difference in L between the FLS and the MFLS G-functions method sizings, versus normalized ground load $Q_{gy}*$ for different maximum design load Q_d a) 80 kW, b) 400 kW, c) 800 kW, borehole spacings B and Darcy velocities

4. Limitations

The proposed methodology for including groundwater flow effect into the sizing of BHEs relies on some hypothesis and simplifications:

1) on the one hand we assumed that the borehole thermal resistance R_b can be calculated neglecting any impact of groundwater flowing around the borehole. This approach is coherent with the outcomes by [16], who numerically calculated R_b for a double U-pipe in a non-permeable grouting for Darcy flows up to 1 m/day in the surrounding ground, and found substantial agreement with values calculated through EED tool on the basis of pure conduction in the ground. More recently Rico and Hermann [17] developed an analytical solution for the heat transfer problem in the inner region of the borehole lapped by creeping flow. They show that, similar to the purely conductive case, it is possible to use a network of thermal resistances, but they depend on the Péclet number and they are sensitive to the pipe legs orientation with respect to the groundwater flow. However, based on their results, it is possible to state that the difference in R_b values compared to the conductive case can be limited to ±3% for $Pé_{r_b} < 0.2$;
2) on the other hand the methodology relies on the accuracy of MFLS g-functions to represent advection and conduction effects on BHE operation; in this regard, it is worth mentioning that, according to the numerical validation of the MFLS g-functions reported in [18], the error associated with the use of G_{MLFS} increases

with Péclet number. However, by adopting as above the condition $Pé_{r_b} < 0.2$, the maximum relative error remains below 5%.

5. Conclusions and prospects

In this paper the classical ASHRAE sizing method was modified in two steps to include groundwater flow in the BHEs design. The application of the improved method to a series of case studies showed that groundwater flow generally reduces the required BHEs size, especially for small borehole spacing and significant unbalanced yearly ground load. At least for the case studies analysed, Darcy velocity equal to 10^{-7} m/s (namely $Pé_{r_b} = 0.013$ considering the parameters adopted) is identified as a threshold value below which the difference in the design of the BHEs compared to the case with null groundwater velocity remains below 20%.

Although promising, the methodology proposed in this study requires further improvements and validations. Firstly, at high Darcy velocity, both the evaluation of the borehole thermal resistance relying on pure conduction and the use of MFLS g-functions are expected to be inaccurate. Based on literature studies, the inaccuracy of these two approaches can be kept below 5% if Péclet is lower than 0.2. However, the Péclet limit below which the present sizing method as a whole can be considered accurate needs to be identified, while more suitable models or corrections are necessary to model groundwater impact on the sizing for larger Péclet numbers. Thus the next step is certainly the validation of the proposed sizing method against detailed numerical simulations, a procedure that will allow also to evaluate the range of groundwater flows where it can be applied. Secondly, to allow an easy application of the improved method that is coherent with the simplicity of the original ASHRAE method, suitable interpolated expressions for the FLS and MFLS g-functions would be useful. Therefore, symbolic regression techniques will be applied to obtain proper simplified equations.

References

[1] Yang H, Cui P, Fang Z. Vertical-borehole ground-coupled heat pumps: A review of models and systems. Applied Energy 2010;87(1):16–27.

[2] Kavanaugh SP, Rafferty K. Ground-Source Heat Pumps - Design of Geothermal Systems for Commercial and Institutional Buildings. Atlanta, USA: ASHRAE; 1997.

[3] Bernier MA, Chahla A, Pinel P. Long-Term Ground-Temperature Changes in Geo-Exchange Systems. 2008;114.

[4] Capozza A, De Carli M, Zarrella A. Design of borehole heat exchangers for ground-source heat pumps: A literature review, methodology comparison and analysis on the penalty temperature. Energy and Buildings 2012;55:369–79.

[5] Fossa M, Rolando D. Improved Ashrae method for BHE field design at 10 year horizon. Energy and Buildings 2016;116:114–21.

[6] Fossa M, Rolando D. Improving the Ashrae method for vertical geothermal borefield design. Energy and Buildings 2015;93:315–23.

[7] Ahmadfard M, Bernier M. Modifications to ASHRAE's sizing method for vertical ground heat exchangers. Science and Technologuìy for the Built Environment 2018; 24:803-817.

[8] Angelotti A, Alberti L, La Licata I, Antelmi M. Energy performance and thermal impact of a Borehole Heat Exchanger in a sandy aquifer: Influence of the groundwater velocity. Energy Conversion and Management 2014;77:700–8.

[9] Piipponen K, Soesoo A, Arola T, Bauert H, Tarros S. Impacts of groundwater flow on borehole heat exchangers: Lessons learned from Estonia. Renewable Energy 2024;237:121448.

[10] Fossa M. The temperature penalty approach to the design of borehole heat exchangers for heat pump applications. Energy and Buildings 2011;43(6):1473–9.

[11] Molina-Giraldo N, Blum P, Zhu K, Bayer P, Fang Z. A moving finite line source model to simulate borehole heat exchangers with groundwater advection. International Journal of Thermal Sciences 2011;50(12):2506–13.

[12] Lamarche L, Beauchamp B. A new contribution to the finite line-source model for geothermal boreholes. Energy and Buildings 2007;39(2):188–98.

[13] Conti P. Dimensionless Maps for the Validity of Analytical Ground Heat Transfer Models for GSHP Applications. Energies 2016;9(11):890.

[14] Philippe M, Bernier M, Marchio D. Validity ranges of three analytical solutions to heat transfer in the vicinity of single boreholes. Geothermics 2009;38(4):407–13.

[15] Cimmino M, Bernier M. A semi-analytical method to generate g-functions for geothermal bore fields. International Journal of Heat and Mass Transfer 2014; 70: 641-650.

[16] Wagner V, Bayer P, Kubert M, Blum P. Numerical sensitivity study of thermal response tests. Renewable Energy 2012; 41: 245-253.

[17] Rico J, Hermanns M. On the network of thermal resistances embodying the response of geothermal boreholes to creeping groundwater flows. International Journal of Thermal Sciences 2024; 204:109222.

[18] Tye-Gingras M, Gosselin L. Generic ground response functions for ground exchangers in the presence of groundwater flow. Renewable Energy 2014; 72: 354-366.